Structure Activity Studies of

Quinones and Analogues

by

Nidhi Raghav

A Thesis Presented in Partial Fulfillment
of the Requirements for the Degree
Master of Science

Approved March 2011 by the
Graduate Supervisory Committee:

Sidney Hecht, Chair
Peter Williams
Ian Gould

ARIZONA STATE UNIVERSITY

May 2011

ABSTRACT

Many natural and synthetic quinones have shown biological and pharmacological activity. Some of them have also shown anticancer activity. Ubiquinone (CoQ_{10}) which is a natural quinone, is a component of the electron transport chain and participates in generation of ATP (adenosine triphosphate). Cellular oxidative stress is key feature of many neurodegenerative diseases such as Friedreich's ataxia, Alzheimer's disease and Parkinson's disease. The increased generation of reactive oxygen species damages cell membranes and leads to cell death. Analogues of ubiquinone in the form of pyrimidinols and pyridinols, were effective in protecting Friedreich's ataxia lymphocytes from oxidative stress-induced cell death. There were some structural features which could be identified that should be useful for the design of the analogues for cellular protection against oxidative stress.

There are quinones such as doxorubicin, daunomycin and topopyrones which have anticancer activity. Here I evaluated topopyrone analogues which poison both topoisomerases I and II. The topopyrone analogues were lethal to human breast cancer cells, but these analogues were not as potent as camptothecin.

ACKNOWLEDGMENTS

I would like to express the deepest appreciation to my advisor, Professor Sidney Hecht. Without his guidance and persistent help, this thesis would not have been possible. He has been a continuous source of inspiration and encouragement. I would like to thank members of my committee Professor Ian Gould and Professor Peter Williams for their support and invaluable guidance in various areas of my thesis.

I would also like to express my sincere appreciation to Dr. Qasim Khan, Dr. Omar Khdour and Dr. Jeffrey Armstrong for providing encouragement and guidance throughout this study. I wish to express my sincere gratitude to my lab members for their assistance, encouragement and friendship.

TABLE OF CONTENTS

LIST OF TABLES

LIST OF FIGURES

ABBREVIATIONS

DNA	deoxyribonucleic acid
OD	optical density
DMSO	dimethyl sulfoxide
DEM	diethyl maleate
DPBS	Dulbecco's phosphate buffer saline
RPMI	Roswell park memorial institute
PMS	phenazine methosulfate
ATP	adenosine 5'-triphosphate
TCA	tricarboxylic acid
CoQ	coenzyme Q
ROS	reactive oxygen species
GSH	glutathione
GSSG	glutathione disulfide
FRDA	Friedreich's ataxia
FXN	frataxin
SDH	succinate dehydrogenase
ETC	electron transport chain
kb	kilobase
M	molar
mg	milligram
µl	microliter
ml	milliliter
°C	degree Celsius

CHAPTER 1

CYTOPROTECTIVE EFFECTS OF ANALOGUES OF COENZYME Q

Introduction

Mitochondria participate in a number of metabolic transformations, including pyruvate oxidation, the Krebs cycle and metabolism of amino acids and fatty acids. The most important function of the mitochondria is generation of ATP by the mitochondrial electron transport chain (oxidative phosphorylation) (*1*). The respiratory chain in the inner mitochondrial membrane has five protein complexes. These are complex I or NADH dehydrogenase-ubiquinone oxidoreductase; complex II or succinate dehydrogenase-ubiquinone oxidoreductase; complex III or ubiquinone cytochrome *c* oxidoreductase; complex IV or cytochrome *c* oxidase; and complex V or ATP synthase (Figure 1) (*2*).

There are two small molecules which carry electron between complexes. Coenzyme Q transfers electron from complex I to complex III and from complex II to complex III. Cytochrome *c* transfers electrons from complex III to complex IV (Figure 1) (*2, 3*).

Energy is released in the mitochondrial matrix from the Krebs cycle (TCA cycle) in the form of NADH and $FADH_2$. Electrons are transferred from NADH to complex I and $FADH_2$ to complex II. The electrons travel down the respiratory chain and are finally accepted by oxygen in complex IV (*3*).

As the electrons transit the respiratory chain, protons are pumped across the inner mitochondrial membrane (from the matrix to intermembrane space)

from complexes I, III and IV. ATP is generated by the transport of these protons back into the mitochondrial matrix through complex V (ATP synthase) (*3, 4*).

Reactive oxygen species (ROS) generation

The mitochondrial respiratory chain is the main producer of reactive oxygen species in the cell. ROS production is increased as a result of respiratory chain dysfunction (*5*). Cellular oxidative damage is an important factor in aging and neurodegenerative diseases (*6*). ROS can damage cellular macromolecules and a suitable defense system is necessary (*6, 7*). The defense system in the cells works to reduce the levels of ROS by expressing and regulating antioxidant enzymes such as superoxide dismutase, glutathione peroxidase and catalase. The defense system is also supported by non-enzymatic antioxidants such as α-tocopherol (vitamin E), ascorbic acid (vitamin C), glutathione (GSH) and vitamin A (*7*).

The short chain hydrophilic quinones show a prooxidant effect in the oxidized state while in a fully reduced state they have an antioxidant effect (Figure 2). For example both CoQ_1 and decylubiquinone are electron acceptors from complex I. But CoQ_1 can enhance oxidative stress as it transfers the electron to molecular oxygen (*5*).

$$2O^{-\cdot}_2 + 2H^+ \rightarrow H_2O_2 + O_2 \quad (1)$$

$$H_2O_2 + 2GSH \rightarrow GSSG + 2H_2O \quad (2)$$

The superoxide formed by mitochondria is acted upon by superoxide dismutase (Equation 1) and converted to hydrogen peroxide. Glutathione peroxidase then converts hydrogen peroxide to water (Equation 2) (*8*).

A variety of factors influence superoxide production by mitochondria. Superoxide production varies with the organism, tissue and age (*9, 10*). For example, in the brain mitochondrial complex I is the main producer of superoxide (*10*).

Mitochondrial ROS production increases under conditions of low oxygen concentration. In cultured cells, when the oxygen concentration is lowered to 1-3% (normal value 21% oxygen) ROS generation increases (*9*).

There is production of ROS by the mitochondria in both normal and diseased cells. There is generation of $O_2^{\cdot -}$ in the mitochondrial matrix and intermembrane space. The main sites of superoxide formation during oxidative phosphorylation are complexes I and III. The major potential sites of ROS production were identified by using inhibitors of complexes I and III. In presence of complex I or complex II substrates, mitochondria did not produce significant amounts of superoxide or hydrogen peroxide, but the production of oxygen radicals increased considerably in the presence of inhibitors. When inhibitors are added the respiratory complexes become strongly reduced and generate ROS. Complex I generates ROS primarily in the matrix side of the inner membrane of mitochondria while complex III generates superoxide towards the intermembrane space (*11*).

The rate of radical generation seems to be lower in long-lived animals in comparison to short-lived animals as suggested by comparative studies in different species. There are results suggesting that ROS generation is under the

control of genotype of the organism instead being a mere by-product of mitochondrial respiration (*12*).

Under physiological conditions the superoxide produced by complexes I and III is converted to H_2O_2 with the help of enzyme manganese superoxide dismutase (MnSOD) present in the mitochondrial matrix (*9*). Superoxide can cross the mitochondrial membrane in an uncharged form (*13*). If there is significant amount of superoxide remaining in the matrix, it can oxidize and inactivate iron-sulfur cluster containing enzymes. The superoxide generated in the intermembrane space is dismutated to H_2O_2 by the enzyme copper zinc superoxide dismutase (Cu/Zn SOD) (*8*). In addition to ROS production by the electron transport chain in the inner mitochondrial membrane, the outer membrane is a large source of H_2O_2 production by oxidative deamination of amines by monoamine oxidase (*14*).

The generation of superoxide and peroxide radical in the inner mitochondrial membrane is close to redox pools of Cu and Fe. The proximity provides feasible conditions for Fenton chemistry leading to hydroxyl radical ($^{\bullet}OH$) formation. The $^{\bullet}OH$ radical reacts with the deoxyguanosine base of mitochondrial DNA to form 8-hydroxydeoxyguanosine. Hydroxyl radical ($^{\bullet}OH$) inactivates mitochondrial enzymes such as NADH dehydrogenase, NADH oxidase, succinate dehydrogenase and ATPase (*14*). Peroxides can also induce peroxidation of cellular lipids and damage cellular membranes (*15*).

The peroxide concentration in the cells is kept at a low level with the help of glutathione peroxidase (GPX). GPX reduces hydrogen peroxide to water by 2

e^- transfer from GSH to produce GSSG (*16*). Glutathione is synthesized in the cytosol by the condensation of cysteine and L-glutamate to form γ-glutamylcysteine, catalyzed by γ-glutamylcysteine synthetase in the rate limiting step. Glutathione synthetase then adds glycine to the C terminus. It is exported from the cytosol to the mitochondria by dicarboxylate and 2-oxoglutarate transporters present in the inner mitochondrial membrane (*16*). The glutathione in the cells can be depleted experimentally by diethyl maleate, ethyl methanesulfonate and various other chemicals (*15*).

Mitochondrial ATP production declines when there is substantial increase in ROS formation. There is excessive release of Ca^{2+} into the cytosol which is taken up by mitochondria and the mitochondrial permeability transition pore (MPTP) is activated. Upon activation it opens a channel in the inner membrane leading to destruction of the electrochemical gradient and ATP synthesis. This initiates programmed cell death (*16*). MPTP regulation can vary with different tissue. Not all of the ubiquinone analogues which inhibit MPTP prevent cell death. However, all MPTP-inducing ubiquinones induce cell death. MPTP regulation does not correlate with regulation of ROS production (*17*).

Coenzyme Q_{10} (CoQ_{10})

CoQ_{10} is mainly found in humans. CoQ_{10} is present in excess compared to other components of the respiratory chain. CoQ_{10} content decreases with age normally. It can act as both prooxidant and antioxidant (Figure 2). CoQ_{10}, when close spatially to complexes I and II, accepts electrons and gets reduced, then transfers electrons to complex III. Reduced CoQ_{10} can also react with molecular

oxygen to produce superoxide if it is close to oxygen (Figure 2). The partitioning of the quinone molecule in the cell between membrane cores, surface and soluble phases determines its efficiency as an antioxidant (*18*). In presence of an inhibitor such as antimycin, a complex III inhibitor, electrons cannot progress in the respiratory chain and get redistributed, resulting in formation of unstable ubisemiquinone. This can lead to superoxide formation. CoQ_{10} is very hydrophobic so it shows an affinity for lipoperoxide or tocopheryl radicals (*19*).

CoQ_{10} and its analogues can be used to treat primary CoQ_{10} deficiency due to defects in ubiquinone biosynthesis (*19*). CoQ_{10} deficiency symptoms are sometimes seen with encephalomyopathy, Leigh syndrome, severe multisystem infantile disease, cerebellar ataxia, or myopathies. These patients have benefited from CoQ_{10} supplementation (*16*). CoQ_{10} supplementation can be used to normalize the bioenergetic status and oxidative balance in fibroblasts of CoQ_{10} deficient patients. After 24 hours of CoQ_{10} supplementation the fibroblasts deficient in CoQ_{10} do not show an improvement in ATP levels or in ATP/ADP ratios. However after one week of treatment, CoQ_{10} increases ATP levels and improves the ATP/ADP ratio. This can be explained by the strong lipophilic nature of CoQ_{10} (*19, 20*). It accumulates in the membranes of lysosomes, the endoplasmic reticulum and the plasma membrane due to its lipophilicity. A small portion (~11%) reaches mitochondria, but only a portion of this reaches the inner membrane to take part in the respiratory chain as some of it gets trapped in the outer membrane (*19*).

Idebenone

The benzoquinone ring of idebenone can undergo reversible reduction and oxidation reactions. Idebenone is a synthetic compound with possible prooxidant and antioxidant properties (Figure 2). Idebenone can be readily oxidized by mitochondrial complex III (Figure 3) and is reduced by complex I, complex II and glyceraldehyde-3-phosphate dehydrogenase (*21*). It can interact with other redox compounds including CoQ_{10} in the mitochondrial respiratory chain. It increases the level of ROS in the cells in the presence or absence of complex I inhibitor rotenone (*5*, *22*). Idebenone crosses the blood-brain barrier. It has been used in clinical trials to treat Alzheimer disease and Friedreich's ataxia (*16*).

Decylubiquinone

Decylubiquinone (2, 3-dimethoxy-5- methyl-6-decyl-1, 4-benzoquinone) is a synthetic ubiquinone analogue. It is a hydrophobic quinone that has a 10-carbon side chain that enables it to pass through mitochondrial membranes. It accepts electrons from complexes I and II and transfers them to complex III. Oxygen consumption is taken as a measure of efficiency of respiratory chain. It was observed in nerve synaptosomes that on inhibition of complex I there was 40% synaptosomal oxygen consumption. However, in presence of decylubiquinone there was 70% oxygen consumption. Decylubiquinone increased the inhibition thresholds for complexes I/III, II/III and III, when myxothiazol was used to inhibit complex III (*23*).

Complex I has the most complicated structural organization. It is also the rate determining step of the respiratory chain. Complex I in the respiratory chain

donates electrons to the CoQ_{10}. CoQ_{10} is a hydrophobic molecule and is localized in the hydrophobic core of the lipid bilayer (*24*). The NADH coenzyme Q oxidoreductase (complex I) catalyzes the reduction of CoQ_{10} by NADH. The binding site of coenzyme Q is initially small. However, NADH binding to the enzyme leads to a conformational change in the coenzyme Q binding site. This enables the site to accept coenzyme with larger side chains such as decylubiquinone (*25*). Complex I is inhibited by number of compounds (*24*). Both the benzoquinone ring and the alkyl side chain of the CoQ are essential for electron transfer and binding (*26*). The antioxidant efficiency of quinones depends on the targeting of quinones to the site of free radical production in the mitochondrial inner membrane (*22*). The analogues should bind to the sites on complexes I and III located deep within the hydrophobic core of membrane (*26*).

Mitochondrial disease

A number of genetic mutations can cause mitochondrial dysfunction. The mitochondrial defects can affect vital organs of the body. Friedreich's ataxia (FRDA), Alzheimer's disease, Parkinson's disease, amyotrophic lateral sclerosis and Huntington's disease are some of the disease due to mitochondrial dysfunction and impairment of energy production (*27, 28*). In this study we are focusing on Friedreich's ataxia (FRDA). It is a neurodegenerative and cardiodegenerative disease believed to arise from an insufficiency of the protein frataxin. It is characterized by progressive ataxia, speech problems and heart disease (cardiomyopathy) (*29*).

Frataxin is a nuclear-encoded protein targeted to the mitochondrial matrix (*30*). Most FRDA patients are homozygous for GAA triplet repeats within the first intron of the frataxin gene (*31*). Normal alleles have between 6-34 GAA repeats, while in FRDA patients there are between 70-1700 GAA triplet repeats. This results in reduced amounts of frataxin protein. This may be because the GAA/TTC repeats form unusual DNA structures, like DNA triplexes which block transcription. There is an inverse relationship between the size of GAA repeat and the age of onset of the disease (*32*). Some patients were found to have point mutation in the frataxin gene, located on chromosome 9 (*31*).

Frataxin acts as cofactor for proteins involved in mitochondrial electron transport chain and may interact with mitochondrial aconitase affecting energy metabolism. It is responsible for assembling Fe-S cluster in proteins with this prosthetic group. Frataxin is also involved in iron binding and storage (*30*). Frataxin has an additional role in iron detoxification and regulates oxidative stress. Frataxin deficiency sensitizes cells to oxidative stress and subsequently cell death (*30*).

Iron sulfur clusters are an important part of the respiratory complexes and frataxin plays an important part in biogenesis of iron-sulfur cluster. They are synthesized in mitochondria by a complex pathway which is being elucidated (*33*). The biosynthesis starts with release of elemental sulfur from cysteine with the help of enzyme cysteine desulfurase. The elemental sulfur is incorporated into a scaffold protein. The two forms of frataxin present in the normal cells in steady are $FXN^{81-210}$and FXN^{42-210}. FXN^{81-210} donates Fe^{2+} for iron-sulfur cluster

assembly on the iron-sulfur cluster scaffold protein. FXN^{42-210} can donate either Fe^{2+} or Fe^{3+} (*33*). The initial structure is a 2Fe-2S tetrahedral-like complex which is followed by 3Fe-4S and 4Fe-4S clusters. Iron sulfur cluster play chemically diverse role. Fe-S clusters in complex I and succinate dehydrogenase (SDH) help in catalyzing electron transfer reactions from NADH and $FADH_2$. The association of the iron sulfur cluster with the respiratory chain enzymes helps in electron transfer by the enzyme and prevents electron leakage to molecular oxygen. Thus the generation of ROS is avoided (*7*).

Results

We want to find CoQ analogues which can act as antioxidants and prooxidants and also support oxidative phosphorylation by transporting electrons through the ETC. The analogues would prevent damage to the mitochondrial membranes and oxidative stress to the cells.

We started by evaluating our analogues in CEM leukemia cells. These cells were in the log phase of the growth. They were treated with 5 mM diethyl maleate (DEM) to deplete cellular glutathione (*15*). CEM cells were treated with DEM for four hours. Upon depletion of cellular glutathione the cells were subjected to oxidative stress, which resulted in cell death. But when the cells were pretreated with the analogues, they were protected from oxidative stress to varying extents. This cytoprotective effect was determined by measuring the viability of the glutathione depleted cells after 18 hours of drug treatment.

The analogues described in Tables 1-3 share a common substructure, namely 2, 3-dimethoxy-5-methyl-1, 4-benzoquinone. These analogues have different alkyl side chains at the 6-position. The alkyl side chains were different in length, polarity and degree of unsaturation. There were also changes made to the benzoquinone core, but the side chain was same as that of idebenone (**1**) (Table 2). The analogues were analyzed on the basis of their cytoprotective activity. Table 1 summarizes the cytoprotection conferred by compounds **1-5** at concentrations 0.1- 10 μM to the leukemia cells. These compounds are compared to idebenone in their cytoprotective activity. All these analogues had 10-carbon side chains attached at the 6-position.

For all the compounds the cytoprotection generally increased with an increase in drug concentration upto 5 µM concentration. At 10 µM concentration the cytoprotection started declining for some of the compounds (compounds **1**, **2** and **5**). These compounds might be inhibiting the respiratory chain. The extent of increase in cytoprotection varied with different compounds. Among these derivatives, compound **4** having an azido group showed cytoprotective activity of 90% at 5 and 10 µM drug concentrations. This was greater than the cytoprotective activity of idebenone at these concentrations. But compound **4** showed less cytoprotection at 0.1 µM and 0.5 µM concentrations.

Further changes were made to the benzoquinone core (compounds **6**-**8**) (Figure 4). The methoxyl groups at the 2 and 3-positions of the benzoquinone ring were replaced with methyl groups. This change altered the cytoprotective effect of the compounds (Table 2). In case of compound **6,** where both the methoxyl groups were replaced with methyl groups the cytoprotection was improved. Replacement of one methoxyl group (**7** and **8**) gave intermediate results.

The CEM leukemia cells were pretreated with compounds **9**-**15** at concentrations of 0.1-5.0 µM and then depleted of glutathione. These compounds are compared to decylubiquinone in their cytoprotective activity in leukemia cells (Table 3). These analogues with non-polar side chains attached at C-6 of the benzoquinone ring showed better cytoprotective activity than the ones with polar substituents on the side chains. These compounds had modifications to the non-polar side chain. The cytoprotection increased with the increase in drug concentration. At 0.1 µM concentration compound **9** (decylubiquinone) showed

68% viability and compound **10** showed cytoprotective activity of around 45%. At 0.5 μM drug concentration most of the compounds showed > 50% cytoprotection. The structure of the side chain seems to play an important role in determining the cytoprotective activity of the compounds. Compounds **11** and **12** (Figure 5) differ only in the length of the side chain attached at the C-6 position of the benzoquinone ring, but compound **12** showed less cytoprotection than compound **11**. The compounds **13** and **15** having a double bond at the end of the alkyl side chain showed cytoprotection similar to decylubiquinone at 0.5, 1.0 and 5 μM concentration. The branched side chain compound **14** showed somewhat less cytoprotection at 0.5 μM concentration in comparison to decylubiquinone. The compounds differing in the length of the side chain were highly effective in protecting cells under oxidative stress (Table 4). Compounds having an alkyl side chain of 9 or 10 C atoms were optimal for cytoprotection (Tables 3 and 4). The compounds with a side chain of at least eight carbons maintained 50% viability at a concentration as low as 0.05 μM (50 nM).

Friedreich cells are vulnerable to oxidative stress due to their reduced frataxin levels. When cultured they exhibit cell viability of about 90%. Some pyridinol analogues and idebenone analogues were tested in FRDA cells. The frataxin deficient cells generate more ROS than normal cells (*29*, *30*). The cells were pretreated with the synthesized analogues in the same way as CEM cells. But they were treated for more than six hours. FRDA cells should have been more vulnerable to oxidative stress due to lesser frataxin content. They seem to have adapted to the deficiency and take longer to die when exposed to DEM.

Compound **23** had the same pyrimidinol core as compound **21** but with a methoxyl group attached to the redox core (Figure 6). Similarly, compound **24** had the same pyridinol core as compound **22** but with a methoxyl group attached to the core (Figure 6). Upon analysis of these compounds it was found that compounds **21, 22** and **23** were effective in cytoprotection of the cells: > 85% viability was obtained at a concentration of 0.5 μM under oxidative stress (Table 5).

Further improvements in structure (Table 6) were realized by adding lipophilic side chains to the pyrimidinol core structures analyzed previously (Table 5) to facilitate delivery to the mitochondrial membranes. These compounds were also highly potent (Table 6). When pretreated with these compounds, the cells exhibited > 80% viability under oxidative stress. Compounds **25**, **26** and **27** with methyl groups attached to the core were generally better than respective methoxyl analogues **28** and **29**.

Some of the compounds which showed high potency in maintaining cell viability in CEM cells were further tested in FRDA cells. In FRDA cells these compounds had either similar or better cytoprotective activity (Table 7). Compound **11** and **14** showed better cytoprotection in FRDA cells at 0.1 and 0.5 μM in comparison to cytoprotection in CEM cells. But all the non-polar compounds tested in FRDA cells were very effective in protecting them from oxidative stress.

Discussion

Mitochondrial dysfunction is implicated in a number of diseases such as Friedreich's ataxia, Alzheimer's disease, Parkinson's disease, amyotrophic lateral sclerosis and Huntington's disease (*27*, *28*). The mitochondria are under oxidative stress in the patients suffering from these diseases. The increase in the level of ROS leads to lipid peroxidation and cell death (*13*).

In this study we evaluated the usefulness of quinones or pyrimidinols as potential treatments for mitochondrial diseases. There is a need to synthesize derivatives that restore electron flow and provide additional antioxidant potential. The derivatives should be able to reach the target tissue, then the cells and the mitochondria. They should have lipophilicity appropriate to insert within the mitochondrial inner membrane. They should be able to restore electron flow between the complexes. But neither CoQ_{10} nor any of the analogues studied to date have been able to restore electron flow in case of respiratory chain deficiency (*22*).

There were a number of modifications made to the substituents attached to the benzoquinone or pyridinol core. We wanted to optimize the structure so that the analogues can participate in the electron transport chain and protect against oxidative stress. The analogues should be able to protect the cells against free radical formation due to the defective mitochondrial respiratory chain. The cytoprotective action of the compounds was characterized in CEM leukemia and FRDA cells. The cells produce ROS during oxidative phosphorylation. But this level is controlled by the various antioxidant defense mechanisms in the cell (*10*).

When the cells were depleted of glutathione by treatment with 5 mM DEM, the cells produced increased ROS. This was followed by lipid peroxidation and cell death (*15*).

We analyzed the effect of the side chain attached at the C-6 position of benzoquinone core. When polar side chains were attached, most of the analogues did not offer much protection against oxidative stress when the cells were depleted of glutathione. In contrast, most of the analogues with non-polar side chain sustained the viability of the glutathione depleted cells. The polar compounds probably could not travel through the lipophilic membranes to reach the mitochondrial inner membrane.

Among the non-polar compounds we analyzed the effect of different modifications in the side chain. We observed variable activity on changing the size of the side chain. The side chains having lengths of more than nine C-atoms were effective in protecting the cells under oxidative stress. Upon introduction of a benzyl or phenyl group at the end of the 10-C chain, the analogues exhibited more than 90% cytoprotection at 5 µM concentration. Compound **12,** with a side chain of 12 C atoms having a phenyl group at the end of the chain was not as effective in protecting cells under oxidative stress. The length of the side chain may not be appropriate for cellular uptake and retention of the compounds in the mitochondrial membranes. The side chain is an important factor in the antioxidant activity of the analogues. The introduction of a double bond at C-10 did not have much effect in comparison to its saturated counterpart. A branched chain caused a small decrease in the cytoprotective activity in comparison to straight chain.

We aim to restore normal mitochondrial function and control the pathophysiology of the diseases caused by oxidative stress. In this study we used cells from FRDA patients. These cells are under oxidative stress due to frataxin deficiency (*31*). Lymphocytes from FRDA patients die after glutathione depletion by treatment with DEM (*34*). But cell death can be prevented by treating the cells with our CoQ analogues. The FRDA cells on pretreatment with pyrimidinol and non-polar benzoquinone analogues when exposed to oxidative stress retained high cell viability (Tables 5, 6 and 7).

Materials and methods

Diethyl maleate (DEM) was purchased from Sigma Aldrich (St. Louis, MO). Trypan blue and cell counter chamber slides were from Invitrogen (Carlsbad, CA).

Cell culture and media: CCRF-CEM cells (ATCC, CCL-119) were grown in RPMI-1640 medium (Gibco, Grand Island, N.Y.) with 10% fetal bovine serum (Hyclone, South Logan, Utah) and 1% penicillin-streptomycin solution (Cellgro, Manassas, VA). We obtained Friedreich ataxia patient lymphocytes from Coriell cell repositories (Camden, N.J., catalog number GM15050E). These cells were cultured in RPMI-1640 medium with 15% fetal bovine serum and 1% penicillin-streptomycin solution. Cells were grown in culture flasks and incubated at 37 °C in a humidified atmosphere of 5% CO_2 in air. Cells were passaged regularly to maintain them in log phase.

Assay for cytoprotection of CEM cells: The viability of the cells depleted of glutathione gives a measure of the cytoprotective activity of the synthesized compounds. Cells were depleted of glutathione (GSH) by treatment with DEM. Cell viability was determined by trypan blue exclusion assay (*35*). When the cell membrane is not intact trypan blue enters the cells, and the cells look blue when seen under a microscope. This allows us to differentiate dead cells vs. live cells. Live cells have intact membranes so trypan blue can not enter these cells.

CEM leukemia cells were grown in RPMI medium 1640 supplemented with 10% fetal bovine serum and 1% penicillin-streptomycin solution. In a 12-well cell culture plate 5×10^5 cells per well were seeded and treated with the test

compounds. The cells were incubated at 37 °C in a humidified atmosphere of 5% CO_2 in air for 18 h. The stock solution of the compounds was prepared in DMSO. Cells were treated with 5 mM DEM for 4 h at 37 °C in a humidified atmosphere of 5% CO_2 in air. The viability of the cells was measured by staining with 0.4% trypan blue solution. Cell suspension and trypan blue were mixed in equal volumes (10 μL). The cells were pipetted into a hemocytometer and the cells were counted. Viable cells excluded the dye and nonviable cells took up the dye. After 4 h more than 90% of the cells treated with only DEM took up the dye and stained blue. Cell viability was calculated as percentage of positive control (cells + media alone). Data is expressed as mean ± SD (n= 3, n is number of readings used to determine mean).

Assay for cytoprotection of Friedreich's ataxia (FRDA) cells: FRDA cells were depleted of glutathione by treatment with DEM. The viability of these cells when pretreated with the synthesized derivatives gave a measure of cytoprotection. Cell viability was determined by trypan blue exclusion assay. FRDA lymphocytes were grown in RPMI medium 1640 supplemented with 15% fetal bovine serum and 1% penicillin-streptomycin solution. In a 12-well cell culture plate 5×10^5 cells per well were seeded and treated with the test compounds. The cells were incubated at 37 °C in a humidified atmosphere of 5% CO_2 in air for 18 h. The stock solution of the derivatives was prepared in DMSO. Cells were treated with 5 mM DEM (diethyl maleate) for 6 h at 37 °C in a humidified atmosphere of 5% CO_2 in air. Cell suspension and trypan blue were mixed in equal volumes (5 μL). After 6 h > 80% of the cells treated with only

DEM took up the dye and stained blue. The positive control (cells not treated with DEM or the analogues) had ~ 90% viability. The cell suspension was pipetted into chambers of cell counter slides. The percentage cell viability in each well was determined using automated cell counter (Invitrogen). Cell viability was calculated as percentage of positive control. Data is expressed as mean ± SD (n= 3, n is number of readings used to determine mean).

Table 1

Cytoprotective effects of compounds **1-5**

Compound	Viable Cells (%)				
	0.1 µM	0.5 µM	1.0 µM	5.0 µM	10.0 µM
1	25 ± 1	36 ± 3	71 ± 1	74 ± 5	53 ± 1
2	19 ± 1	19 ± 1	31 ± 1	57 ± 3	39 ± 3
3	11 ± 0	22 ± 1	43 ± 2	54 ± 4	71 ± 5
4	11 ± 1	21 ± 2	72 ± 2	92 ± 2	98 ± 3
5		14 ± 1	55 ± 4	69 ± 1	48 ± 1

The compounds analyzed are with 2, 3-dimethoxy-5-methyl-1, 4-benzoquinone core and different polar chains at position 6. The CEM cells were pretreated with these compounds and then depleted of glutathione with DEM. Cell viability in the assay is expressed as percentage of positive control.

Table 2

Cytoprotective effects of compounds **6-8**

Compound	Viable Cells (%)		
	0.1 µM	0.5 µM	2.5 µM
1	25 ± 1	36 ± 3	86 ± 4
6	35 ± 3	77 ± 3	96 ± 4
7	23 ± 1	75 ± 8	82 ± 4
8	08 ± 1	21 ± 1	77 ± 1

The compounds analyzed are with 5-methyl-1, 4-benzoquinone core with methyl or methoxyl substituents and hydroxyl side chain at position 6. The CEM cells were pretreated with these compounds and then depleted of glutathione with DEM. Cell viability in the assay is expressed as percentage of positive control.

Table 3

Cytoprotective effects of compounds **9-15**

Compound	Viable Cells (%)			
	0.1 µM	0.5 µM	1.0 µM	5.0 µM
9	69 ± 7	62 ± 3	79 ± 5	87 ± 6
10	43 ± 5	63 ± 4	67 ± 2	92 ± 2
11	10 ± 1	51 ± 5	78 ± 4	94 ± 5
12	19 ± 1	36 ± 5		75 ± 7
13	19 ± 1	83 ± 6	77 ± 4	85 ± 2
14	09 ± 1	43 ± 4	72 ± 2	93 ± 7
15	17 ± 2	69 ± 3	81 ± 4	92 ± 7

The compounds analyzed are with 2, 3-dimethoxy-5-methyl-1, 4-benzoquinone core and different non-polar chains at position 6. The CEM cells were pretreated with these compounds and then depleted of glutathione with DEM. Cell viability in the assay is expressed as percentage of positive control.

Table 4

Cytoprotective effects of compounds **17-20**

Compound	Viable Cells (%)			
	0.01 µM	0.05 µM	0.1 µM	1.0 µM
9	18 ± 2	61 ± 3	69 ± 7	79 ± 5
17	18 ± 1	30 ± 3	41 ± 2	77 ± 5
18	14 ± 1	54 ± 1	68 ± 6	65 ± 7
19	11 ± 1	59 ± 5		81 ± 6
20	18 ± 1	50 ± 5	85 ± 8	84 ± 8

The compounds analyzed are with 2, 3-dimethoxy-5-methyl-1, 4-benzoquinone core and side chains of different length at position 6. The CEM cells were pretreated with these compounds and then depleted of glutathione with DEM. Cell viability in the assay is expressed as percentage of positive control.

Table 5

Cytoprotective effects of compounds **21**-**24**

Compound	Viable Cells (%)		
	0.1 µM	0.5 µM	2.5 µM
21	66 ± 7	89 ± 8	91 ± 8
22	59 ± 5	86 ± 4	90 ± 7
23	62 ± 7	89 ± 6	87 ± 7
24	33 ± 2	32 ± 3	37 ± 4

The compounds analyzed are with pyridinol or pyrimidinol core and hydroxyl side chain at the C-6 position. The FRDA cells were pretreated with these compounds and then depleted of glutathione with DEM. Cell viability in the assay is expressed as percentage of positive control.

Table 6

Cytoprotective effects of compounds **25-29**

Compound	Viable Cells (%)		
	0.1 µM	0.5 µM	2.5 µM
25	50 ± 4	86 ± 4	88 ± 6
26	60 ± 4	87 ± 4	79 ± 5
27	68 ± 1	88 ± 3	93 ± 2
28	45 ± 2	90 ± 2	90 ± 1
29	49 ± 5	71 ± 2	84 ± 4

The compounds analyzed have a pyrimidinol core and side chains of different lengths at the C-6 position. The FRDA cells were pretreated with these compounds and then depleted of glutathione with DEM. Cell viability in the assay is expressed as percentage of positive control.

Table 7

Cytoprotective effects of compounds on cultured FRDA cells

Compound	Viable Cells (%)		
	0.1 µM	0.5 µM	2.5 µM
1	31 ± 1	69 ± 3	95 ± 2
3	26 ± 6	36 ± 5	61 ± 6
9	76 ± 3	83 ± 4	90 ± 6
10	40 ± 3	75 ± 4	90 ± 3
11	59 ± 1	84 ± 1	93 ± 4
14	36 ± 1	85 ± 9	90 ± 5
15	60 ± 3	67 ± 2	92 ± 4
20	76 ± 1	90 ± 4	89 ± 4

The compounds analyzed have the 2, 3-dimethoxy-5-methyl-1, 4-benzoquinone core. These compounds showed high cytoprotective activity in CEM cells. The FRDA cells were pretreated with these compounds and then depleted of glutathione with DEM. Cell viability in the assay is expressed as percentage of positive control.

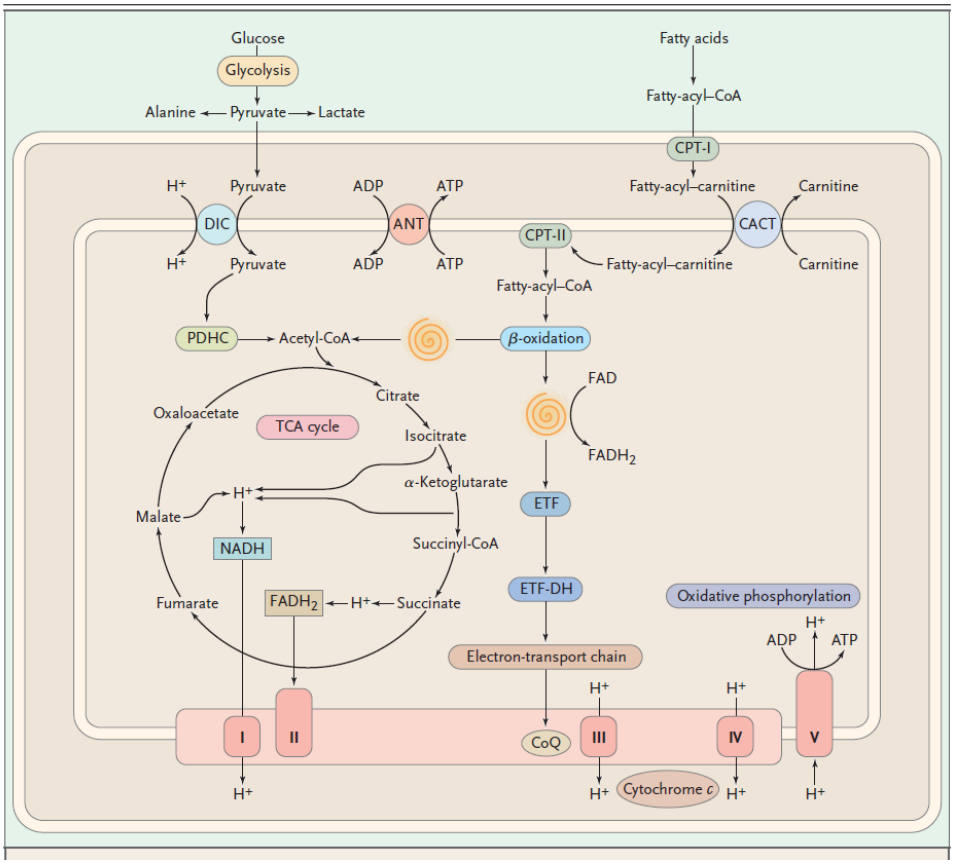

Figure 1: Metabolic pathways operating in mitochondria. The metabolic pathways such as the TCA cycle and oxidative phosphorylation operate in the mitochondrial matrix and inner membrane respectively. The mitochondrial inner membrane has five complexes which participate in ATP formation (*3*).

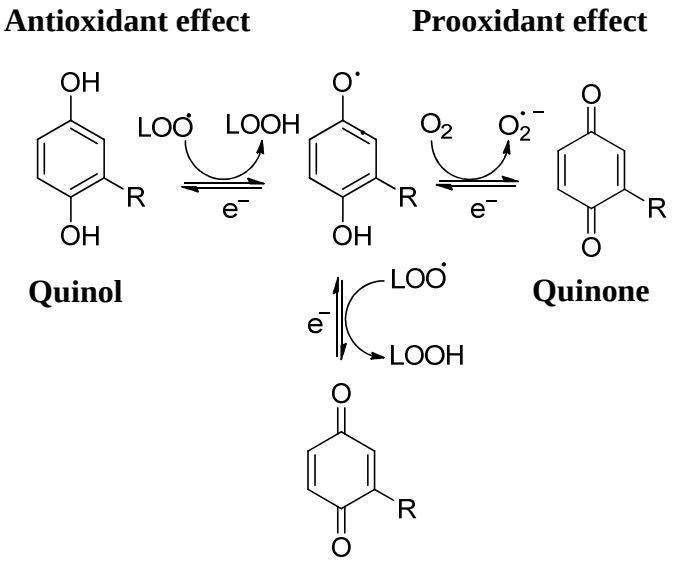

Figure 2: Prooxidant and antioxidant reactions by quinones. The quinol form which is fully reduced has antioxidant effect. The semiquinone can react with oxygen to give toxic radicals. The quinones are reduced by dehydrogenase in the mitochondrial membrane (*22*).

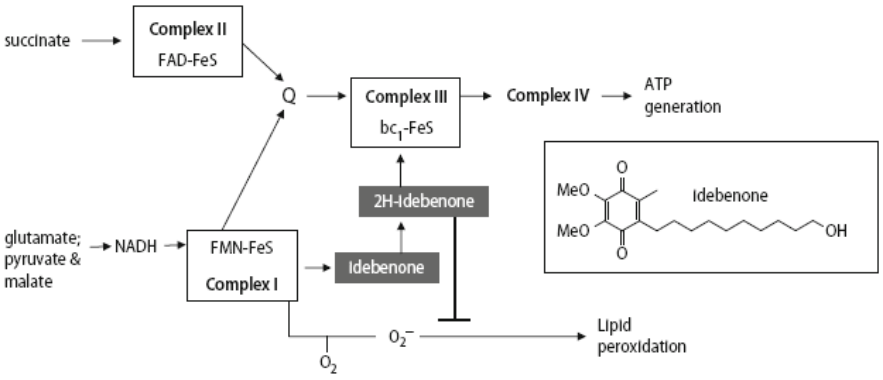

Figure 3: Idebenone as electron carrier in the electron transport chain. Metabolic pathways such as oxidative phosphorylation operate in mitochondria. The mitochondrial inner membrane has five complexes which participate in ATP formation. Idebenone transfers electrons from complex I to complex III (*21*).

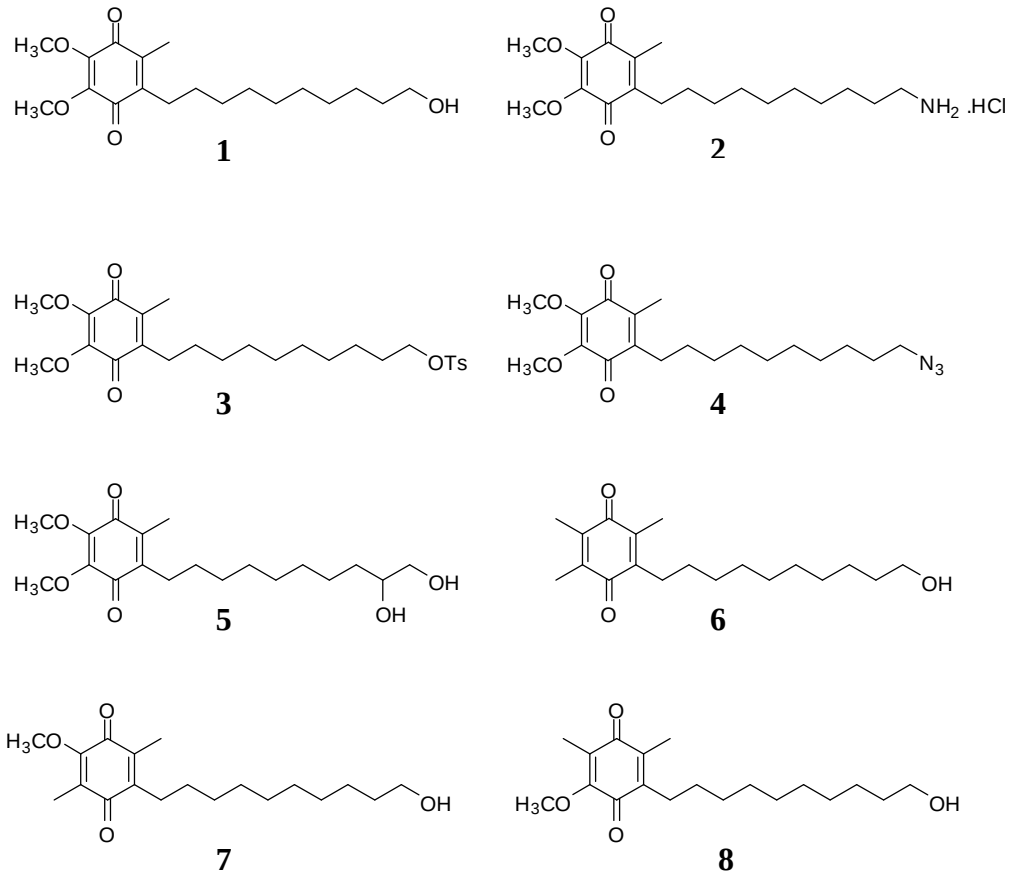

Figure 4: Analogues **1-8** tested for cytoprotective effects. The compounds have 2, 3-dimethoxy-5-methyl-1, 4-benzoquinone core and different polar groups at position 6. (These analogues were synthesized by David Fash. Idebenone was synthesized by Pablo Arce.)

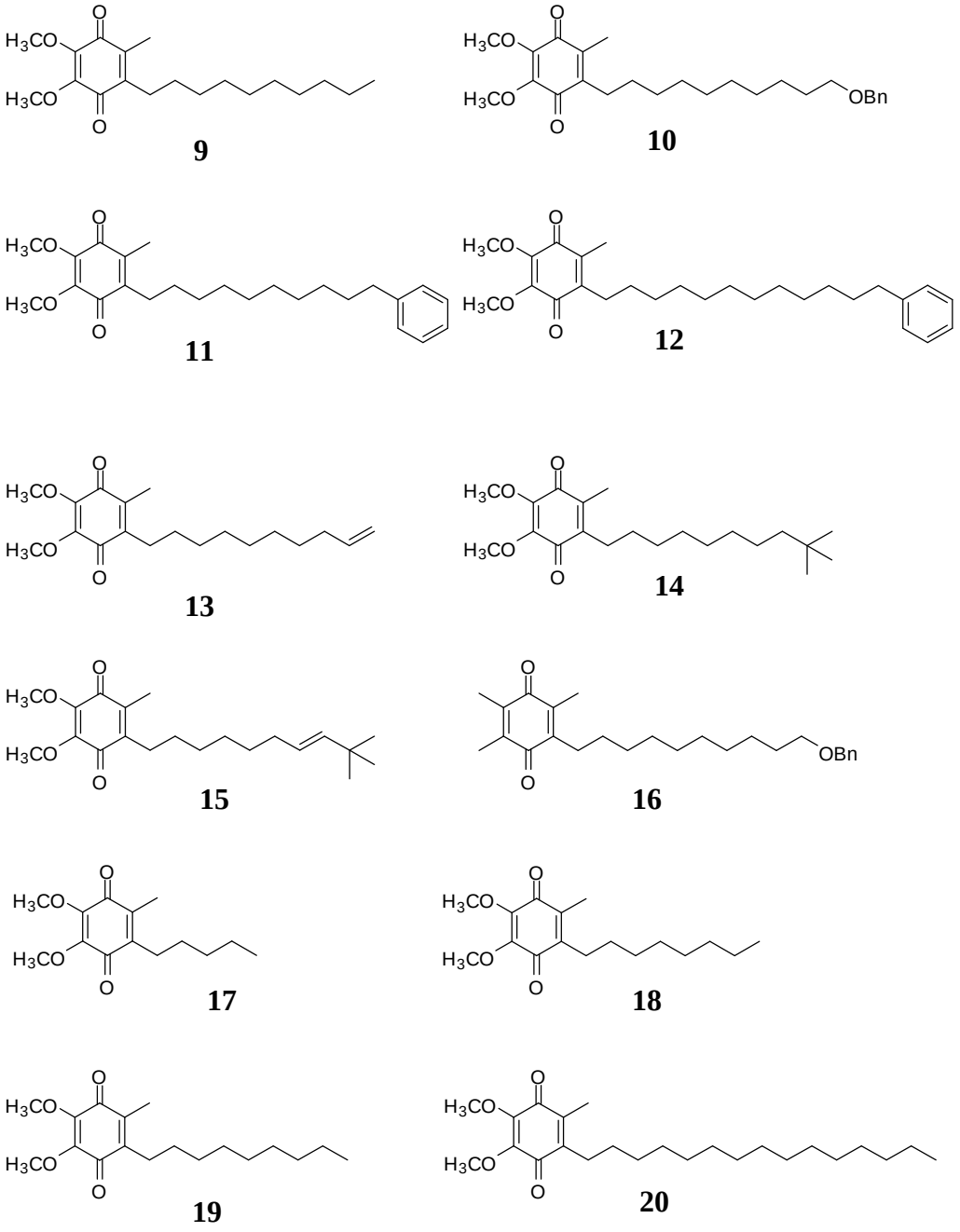

Figure 5: Analogues **9-20** tested for cytoprotective effects. The compounds are with 2, 3-dimethoxy-5-methyl-1, 4-benzoquinone core and different non-polar chains at position 6. (These analogues were synthesized by David Fash.)

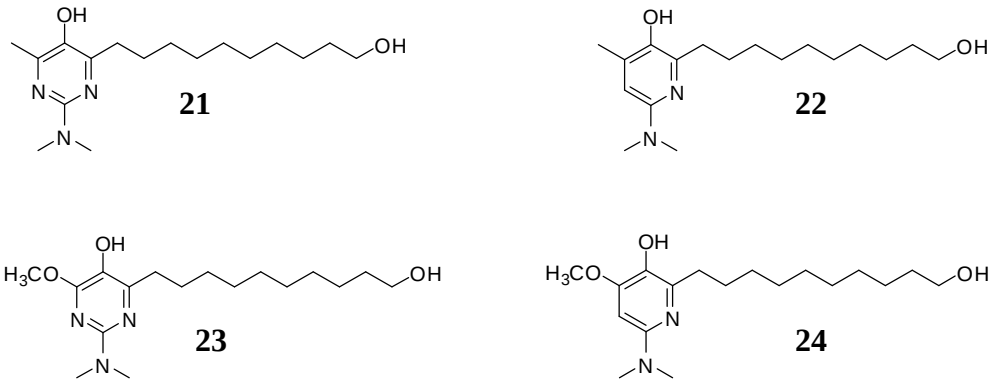

Figure 6: Analogues **21-24** tested for cytoprotective effects. The compounds are pyridinol and pyrimidinol analogues with polar side chains. (These analogues were synthesized by Pablo Arce.)

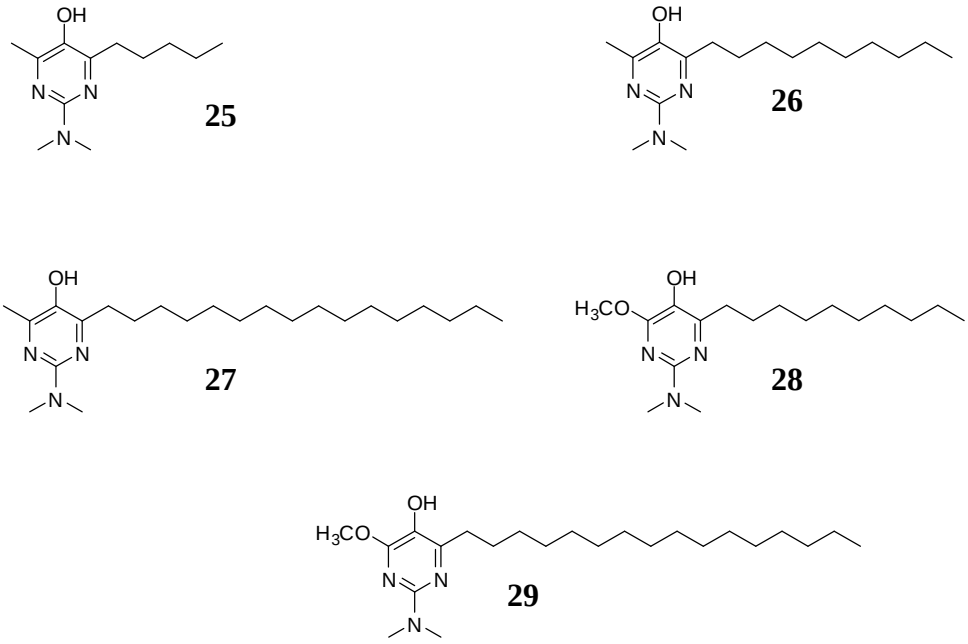

Figure 7: Analogues **25**-**29** tested for cytoprotective effects. Pyrimidinol analogues are with non-polar side chains. (These analogues were synthesized by Pablo Arce.)

CHAPTER 2

CYTOTOXIC ACTIVITY OF TOPOPYRONE ANALOGUES

Introduction

The two strands of DNA need to be separated to serve as a template for transcription, replication, recombination and repair. There is limited free rotation about the DNA helix. Supercoiled DNA relaxation is carried out by DNA topoisomerases (*36*).

DNA topoisomerase I is essential in mammals. Topoisomerase I relaxes the DNA by nicking on a single strand. The broken strand then rotates around the topoisomerase I bound DNA strand. After relaxation has occurred, topoisomerase I religates the break (*36*). Topoisomerase I mediated DNA strand cleavage involves a nucleophilic attack by the active site tyrosine OH group on the DNA phosphodiester bond. This results in breakage of the DNA phosphodiester backbone at the site of cleavage and formation of a phosphotyrosine bond between the enzyme and DNA (Figure 8). This intermediate is termed as 'covalent binary complex' (*37*). The nicks are transient and the religation requires that the 5′-hydroxyl end of DNA aligns with the tyrosine-DNA phosphodiester bond (*36*). The enzyme does not require ATP for the relaxation process.

Topoisomerase II produces transient double stranded breaks in DNA (Figure 9). This enzyme requires energy from ATP hydrolysis. There are two subclasses of this class of enzyme, that is type IIA and type IIB. The type IIA enzyme is present in all bacteria, eukaryotic organisms, some viruses and archaea. The type IIB enzyme is present in all archaea, plants, algae, and few bacteria.

Mechanistically, the type IIB enzyme differs from type IIA DNA topoisomerase. Type II B strictly requires ATP for DNA cleavage. DNA cleavage by the type IIB enzymes generates two-nucleotide 5' protruding ends instead of four-nucleotide overhangs for type IIA enzymes (*38*).

Each nucleotide binding pocket in topoisomerase II also contains one Mg^{2+} and two water molecules. DNA cleavage by topoisomerase II involves a transesterification reaction in which a covalent DNA-protein bond is formed. The cleavage produces staggered ends. Each of two tyrosyl residues in the enzyme makes a covalent linkage to a 5' phosphoryl group of DNA. Topoisomerase II enzyme binds to a duplex DNA (the G segment). The second DNA (the T segment) is bound by the enzyme as the ATP-binding domains dimerize in the presence of ATP. The G segment is cleaved to allow passage of the T segment. The T segment is released through the C-terminal dimer interface and the G segment is then religated (Figure 9). Hydrolysis of ATP and release of the hydrolysis products resets the enzyme to its initial state (*39*).

Topoisomerase inhibitors

Topoisomerase inhibitors could in principle bind either to DNA, to the enzyme or to both. The DNA binding site for topoisomerases involves 15-19 neocleotides (*40*). The binding starts with recognition of small segment (~ 5 base pairs) followed by conformational changes to bind with the entire site (*41*, *42*). The mode of action of topoisomerase inhibitors involves competing with enzyme in the initial recognition step or preventing conformational changes in the enzyme upon DNA cleavage, strand passage (for topoisomerase II) and DNA religation.

The inhibitors that selectively affect religation of the DNA cause the enzyme to become a DNA damaging agent. These inhibitors are designated as poisons. Camptothecin is an example of a topoisomerase I poison. Amsacrine, doxorubicin and etoposide are examples of topoisomerase II poisons (Figure 10b) (*42*). DNA intercalators partially unwind the DNA double helix and distort the structure of DNA around the topoisomerase cleavage site; they prevent religation of the DNA (*42*).

Camptothecin (CPT)

CPT is a pentacyclic alkaloid first isolated by Wall and Wani from the bark of the Chinese tree, *Camptotheca acuminata*. Camptothecin was tested clinically in the mid 1970s and exhibited anti-cancer activity (Figure 10a) (*36*). The primary cellular target of CPT was found to be topoisomerase I (*43*).

CPT specifically binds to the enzyme−DNA complex acting as an uncompetitive inhibitor (*44*). Camptothecin penetrates vertebrate cells readily and targets topoisomerase I. Camptothecin binds reversibly to the topoisomerase I covalent binary complex (*43*). Camptothecin and its derivatives have a relatively low affinity for the topoisomerase I covalent binary complex, as micromolar drug concentrations are required to detectably trap topoisomerase I cleavage complex in biochemical assays (*36*).

Topoisomerase I covalent binary complex with camptothecin has to exist long enough to result in DNA damage. But camptothecin diffuses rapidly from the complex, so a prolonged infusion is needed. Camptothecins produce side

effects such as leucopenia and diarrhea. This limits the dose that can be safely administered, as well as the antitumor efficacy of the drug (*36*).

The lactone form is the active form of the drug (*45*). The α-hydroxylactone within the E-ring of camptothecins is readily converted to the carboxylate form (*46*). The carboxylate form is inactive against topoisomerase I, but it binds tightly to serum albumin. So after administration of the drug, a small portion of the camptothecin is in the active lactone form (*47*). Camptothecin is substrate for drug-efflux pumps (*44*). The cells which overexpress drug efflux pumps display drug efflux-mediated resistance. So, there has been a search to find noncamptothecin topoisomerase I poisons as anticancer drugs (*48*).

Topoisomerase II shows relaxed sequence selectivity of DNA recognition, so it binds at multiple sites to the genome (*49*). Drugs such as etoposide (VP-16), doxorubicin, daunorubicin, amasacrine (m-AMSA), and TAS-103 (Figure 10b) which are topoisomerase II inhibitors prevent DNA religation (*50*). Among these drugs doxorubicin, daunorubicin, amasacrine (m-AMSA), and TAS-103 are intercalators (*51*). Topoisomerase II inhibitors also work without trapping the covalent binary complex. Some DNA intercalators at particular drug concentrations alter DNA structure, preventing topoisomerase II from binding to DNA or from forming a covalent binary complex (*52*). Drugs such as merbarone and bisdioxopiperazines (ICRF 187, 159) inhibit ATP hydrolysis and work without binding to DNA (Figure 11) (*49, 53, 54*). DNA translocation occurs due to error prone repair of topoisomerase II generated DNA double stranded breaks. Topoisomerase II poisons could lead to genetic diseases due to translocation (*55*).

Dual topoisomerase poisons

A number of dual poisons of human topoisomerase I and II have been identified. These include saintopin, intoplicine, pyrazoloacridine, tafluposide, XR 11576 and other benzophenazines (*42*).

The level of topoisomerase I and II enzymes varies between different cell types in the body (*56*, *57*). The expression of topoisomerase I does not change significantly during the cell cycle. On the other hand, the expression topoisomerase II changes through the cell cycle (*58*). Either of these enzymes can support cell division. The resistance to topoisomerase I inhibitors can develop due to downregulation of topoisomerase I. This is accompanied by increase in the expression of topoisomerase II (*59*).

Inhibitors of one topoisomerase partially inhibit topoisomerase activity in the cell. Targeting both the enzymes would potentially improve antitumor activity as topoisomerase I and topoisomerase II have some functions that either can perform. It would also be helpful in case of drug resistance as it would be difficult to resist two enzymes. If the cells show resistance to topoisomerase I inhibitors, they would be more susceptible to topoisomerase II inhibitors. The cells become more dependent on topoisomerase II for carrying out essential DNA functions (*55*).

Natural Topopyrones A, B, C and D

Topopyrones A, B, C and D were first isolated from culture broths of fungi, *Phoma* sp. BAUA2861 and *Pencillium* sp. BAUA4206 by Kanzawa *et al.* in 2000. They were reported to be human topoisomerase I poisons (*60*, *61*). The

topopyrones are planar anthraquinones with a fused 1, 4-pyrone ring (Figure 12). Topopyrones stabilized the topoisomerase I covalent binary complex at the same site as camptothecin. Topopyrones were also reported to be topoisomerase II poisons. So, they are dual inhibitors of topoisomerases I and II. VP-16 is a known topoisomerase II poison used clinically as an antitumor agent. The four natural topopyrones were as potent as VP-16 (*62*). An understanding of the mechanism of these dual topoisomerase inhibitors would be interesting and possibly provide insights allowing the design and testing of analogues with improved activity.

Results

Topopyrones are planar anthraquinone polyphenols. They differ by orientation of the 1, 4-pyrone ring fused on the side of the anthraquinone structure. Topopyrones were reported to be dual topoisomerase poisons (*62*). This led to great interest in evaluating the antineoplastic activity of topopyrone analogues. We evaluated the antineoplastic activity of topopyrone analogues in MCF-7 cell line (human breast adenocarcinoma) by performing cytotoxicity assays. In MCF-7 cells, the antineoplastic activity of topopyrone A was greatest among the topopyrones, with an IC_{50} value of 3 ± 0.1 μM (Table 8). Camptothecin was more active than the topopyrones in MCF-7 cells having an IC_{50} value of 0.2 ± 0.02 μM. These trends were similar to reported values (*60*).

It has been reported that the topopyrones are dual topoisomerase inhibitors (*62*). The natural topopyrone analogues showed good cytotoxic activity. We wanted to design compounds with enhanced cytotoxic activity which can also target both topoisomerases I and II.

Topopyrone A was most potent. In order to determine the structure activity relationships in the series, four analogues of topopyrone A were analyzed (**30**-**33**). In case of analogue **30**, the chlorine was replaced by bromine in the 7-position of the anthraquinone ring (Figure 13). This did not improve the cytotoxicity activity (IC_{50} 19 ± 1.6 μM) (Table 9). However, when an additional bromine atom was attached to the anthraquinone ring (Figure 13) the compound became more potent with an IC_{50} value of 7 ± 0.7 μM (Table 9). Analogues **31** and **32**, in which the phenols on the anthraquinone ring were methylated (Figure

13) were also studied. Analogue **31**, having one bromine attached to the anthraquinone ring, showed no cytotoxic activity, while analogue **32** showed rather low activity (Table 9).

Topopyrone B analogue (**34)**, had a chlorine replaced by bromine at the 7-position of the anthraquinone ring (Figure 13). This analogue did not show any cytotoxic activity (Table 9).

Among the topopyrone C analogues, the position of phenols was changed to carbons 5 and 7 on the anthraquinone ring (Figure 14). Analogue **35** (Figure 14) had an IC_{50} value of 17 ± 1.5 μM. In the case of topopyrone analogue **36**, the phenol at position 5 was methylated (Figure 14). The compound did not show any cytotoxic activity at concentrations up to 20 μM (Table 9).

Similarly in the case of topopyrone D analogue **37**, the position of the phenols on the anthraquinone ring was changed to the 5 and 7 positions (Figure 14). This compound had an IC_{50} value of 13 ± 1.8 μM (Table 9).

Discussion

In this work we sought derivatives of topopyrones which are more active than the naturally occurring species. Accordingly changes were made in the substituents or in their positions on the anthraquinone ring system. The effects of these changes were analyzed using a cellular cytotoxicity assay. The cells were exposed to the test compounds for 72 hours. After 72 hours, the cells were analyzed by treating them with MTS, a colorimetric reagent. This colorimetric reagent measures the viability of the cells on pretreatment with the test compounds.

The in vitro antineoplastic activity of topopyrones A, B, C and D was previously reported (*60*). The natural topopyrones inhibited the growth of tumor cell lines, but the inhibition was weaker than that of camptothecin. In HeLa cells, topopyrone A had an IC_{50} value of 0.56 μM. Topopyrones B, C and D showed less activity in HeLa cells, having an IC_{50} values of 3.5, 6.9 and >5 μM, respectively (*60*).

For topopyrone A, replacing chlorine with bromine on the ring led to either reduced (analogue **30**) or no (analogue **33**) cytotoxicity in MCF-7 cells (Table 9). Apparently, phenols at positions 3, 6 and 8 are important as the compound lost its activity upon methylation of the phenols at these positions. Similarly, topopyrone B lost its cytotoxic activity when the chlorine was replaced with bromine on carbon 7 (analogue **34**). This could be due to the fact that bromine is larger than chlorine and alters interaction with the DNA backbone. For topopyrone C, when the positions of the phenols were changed from positions 6

and 8 to positions 5 and 7 there was some increase in activity (analogue **35**). This improved activity was lost when the phenol at position 5 was methylated (analogue **36**). So a polar group at position 5 seems to improve the cytotoxic activity. This can also be seen in case of analogues **32** and **33**. This was further supported by the study of a topopyrone D analogue. Analogue **37** has a phenol at position 5, and showed improvement in activity. So replacing bromine with chlorine on the ring is detrimental to the activity. The presence of a polar substituent at position 5 seems to play an important role.

Topopyrones are planar anthraquinone with two different ring systems. The orientation of pyrone ring in topopyrone A and C is different from the orientation in topopyrone B and D. But we did not see much difference in activity between them. It is possible that the pyrone ring does not interact with the topoisomerase covalent binary complex. The anthraquinone structure could have sites for interaction with the DNA. The cytotoxicity due to topopyrone analogues can be due to their interaction with topoisomerase covalent binary complex. The compounds could also be acting on some other sites in the cells. We do not have much knowledge about their mechanism of action.

Materials and Methods

MCF-7 cells were obtained from the laboratory of Dr. Douglas Lake, SOLS, Arizona State University. MTS (3-(4, 5-dimethylthiazol-2-yl)-5-(3-carboxymethoxyphenyl)-2-(4-sulfophenyl)-2H-tetrazolium) reagent (catalog number G111A) was purchased from Promega. PMS was from Sigma. RPMI media was obtained from Gibco, Grand Island, N.Y. FBS was from Hyclone, South Logan, Utah and 1% penicillin-streptomycin solution was from Cellgro, Manassas, VA. BCA (bicinchoninic acid) reagent was purchased from Thermoscientific, Rockford, IL. DPBS was purchased from Invitrogen.

Cytotoxicity assay

MTS was the colorimetric agent used in the assay. MTS is a green color water soluble compound. MTS is reduced to water soluble formazan in the presence of PMS by dehydrogenases in the living cells. Formazan formed on bioreduction is brown in color and has an absorbance maximum at 490 nm in PBS. MTS solution (4.1 mM concentration) was made in DPBS. The solution was filter sterilized and had a pH in the range of 6.0 to 6.5. PMS solution (3 mM) was made in DPBS. The solution was filter sterilized. Both the solutions were stored in a light-protected container at -20 °C. Before the experiment both the solutions were mixed in the ratio of 20:1 (v/v).

The cells were trypsinized in log phase and the cell density was measured by trypan blue exclusion test (*35*). The cells were seeded in 96 well plates at a density of 3000 cells per well. The analogues were added to the cells in each well after 24 hours. The experiments were done at five different concentrations of the

tested compounds. The experiments were carried out in triplicate. A positive control was maintained with no test compounds. The cells were incubated with the test compounds for 72 hours. In each well, 40 µL of MTS and PMS solution (ratio 20:1, v/v) was added. The cells were incubated for an additional 2 h. The O.D. was measured at 490 nm. The absorbance was proportional to the number of living cells. Cell viability was calculated as percentage of the positive control. Data is expressed as mean ± SD (n=3, n is the number of readings used to calculate mean).

Table 8

Cytotoxicity values of natural topopyrones

Compound	IC_{50} Value (µM)
topopyrone A	03 ± 0.1
topopyrone B	>20
topopyrone C	>20
topopyrone D	>20

Natural topopyrones A, B, C and D were analyzed in MCF-7 cells. The cells were pretreated with these compounds, then their viability was determined using the colorimetric reagent, MTS. MTS is reduced by the live cells to formazan in the presence of electron coupler, PMS. The amount of formazan formed gives us a measure of cell viability. Cell viability at different concentrations was used to determine the IC_{50} value (µM).

Table 9

Cytotoxic effects of topopyrone analogues

Compound	IC_{50} Value (μM)
30	19 ± 1.6
31	>20
32	18 ± 0.4
33	07 ± 0.7
34	>25
35	17 ± 1.5
36	>20
37	13 ± 1.2

The analogues of natural topopyrone were analyzed in cultured MCF-7 cells. The cells were pretreated with these compounds and then the cell viability was determined using the colorimetric reagent, MTS. MTS is reduced by the live cells to formazan in the presence of electron coupler, PMS. The amount of formazan formed gives us a measure of cell viability. Cell viability at different concentrations was used to determine the IC_{50} value (μM).

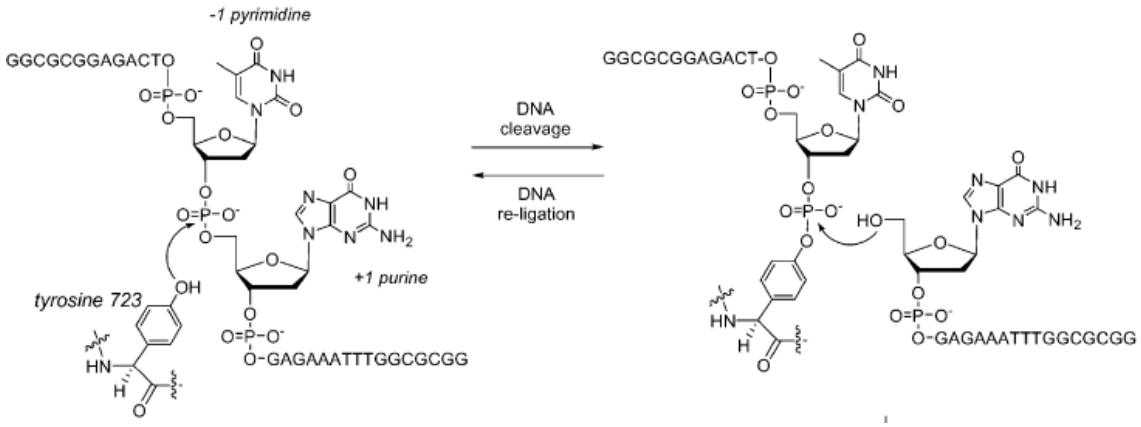

Figure 8: Mechanism of DNA relaxation by topoisomerase I (*37*).

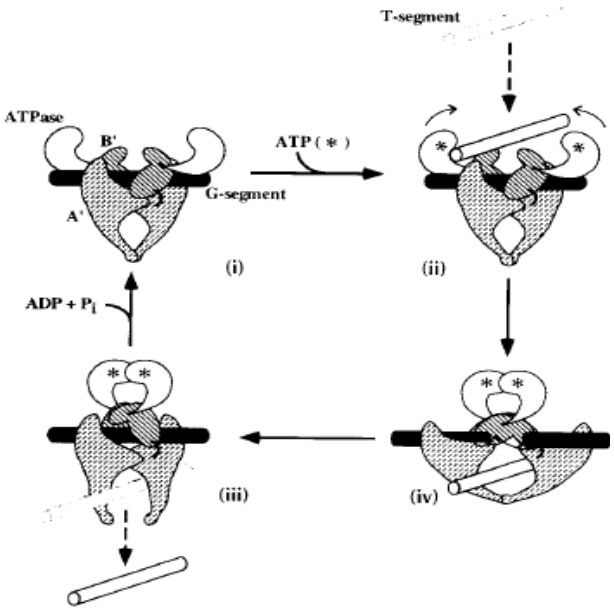

Figure 9: Mechanism of DNA relaxation by topoisomerase II (*39*).

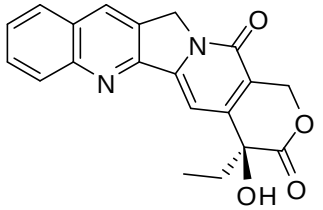

Camptothecin

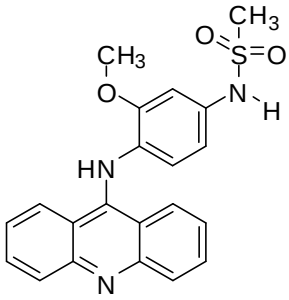

Amasacrine

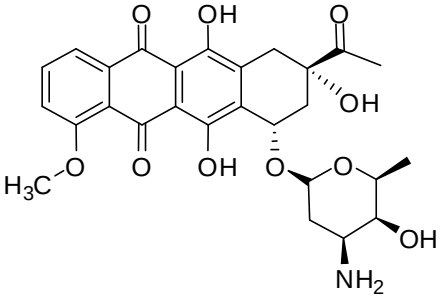

Doxorubicin

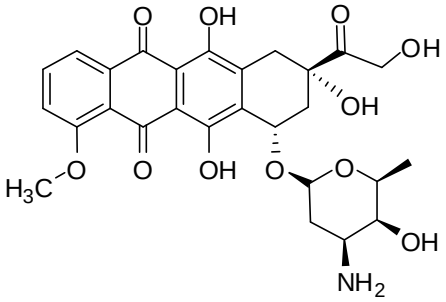

Daunomycin

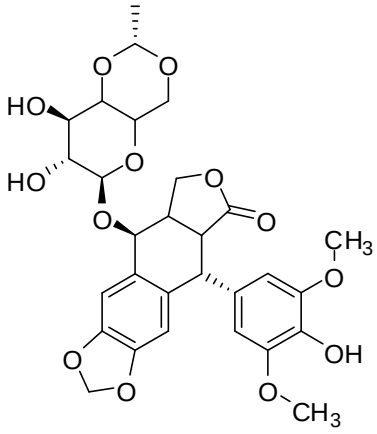

Etoposide

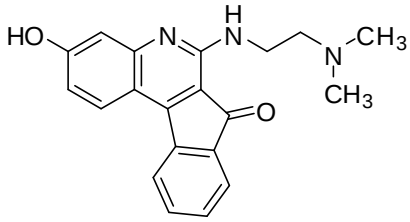

TAS-103

Figure 10**:** Drugs acting as topoisomerase poisons. **a)** Camptothecin stabilizes the topoisomerase I DNA covalent binary complex (*36*) **b)** TAS-103, doxorubicin, daunomycin, etoposide and amasacrine target topoisomerase II (*50*, *55*).

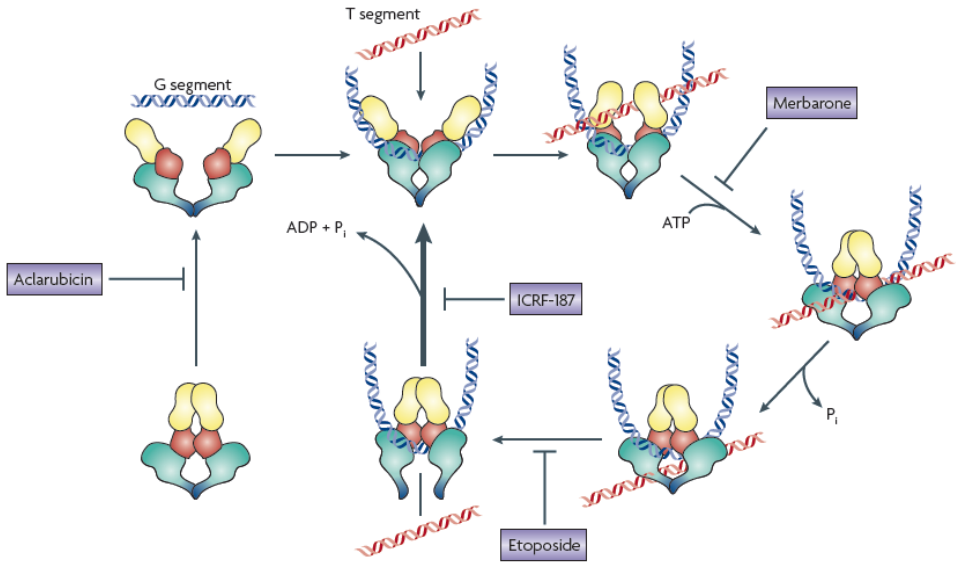

Figure 11: The site of action of topoisomerase II poisons (*49*).

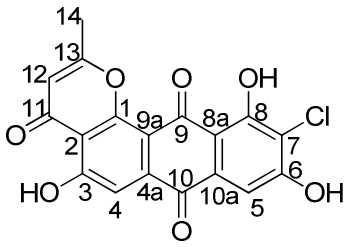

topopyrone A

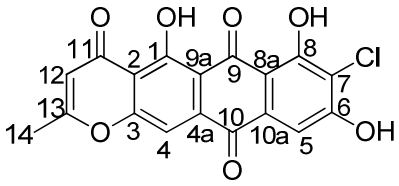

topopyrone B

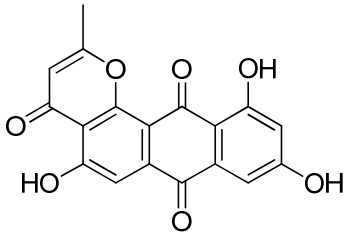

topopyrone C

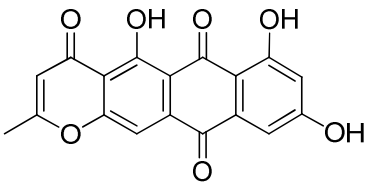

topopyrone D

Figure 12: Structures of natural topopyrones A, B, C and D (*60*). (These compounds were synthesized by Rumit Maini and Simon Leiris.)

Analogues of topopyrone A

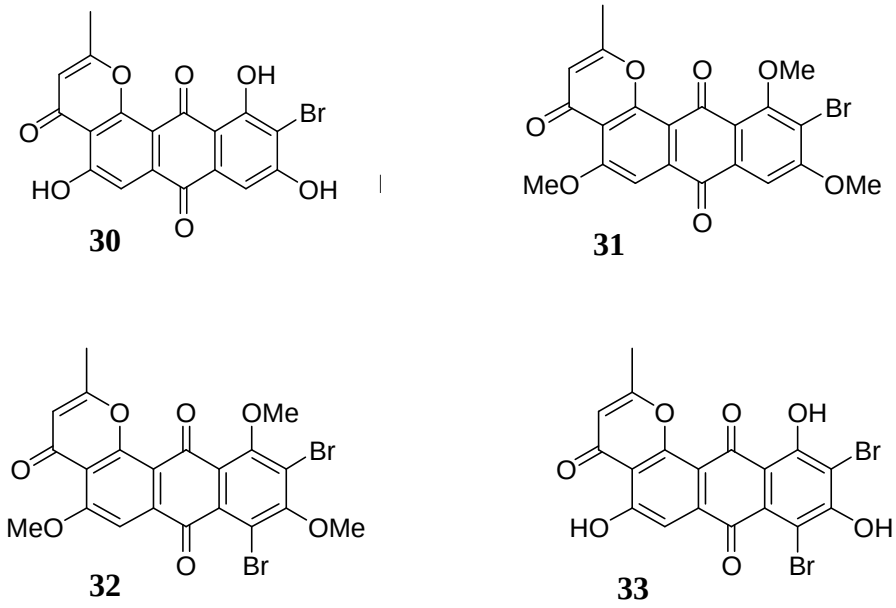

Analogues of topopyrone B

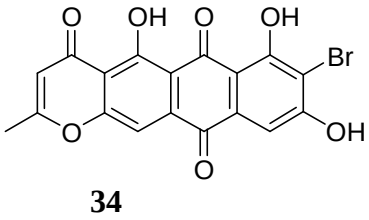

Figure 13: Analogues of topopyrones A and B. Structures of synthesized analogues of topopyrones A and B. (These analogues were synthesized by Rumit Maini.)

Analogues of topopyrone C

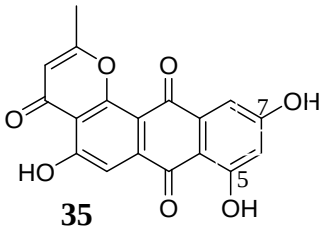

35

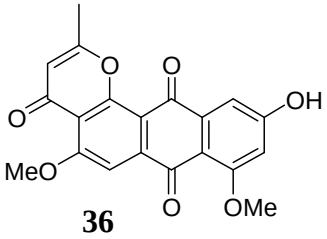

36

Analogues of topopyrone D

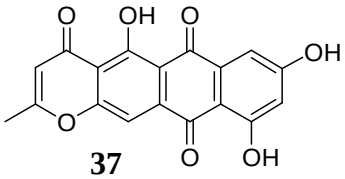

37

Figure 14: Analogues of topopyrones C and D. Structures of synthesized analogues of topopyrones C and D. (These analogues were synthesized by Rumit Maini.)

REFERENCES

1. Mitchell, P., and Moyle, J. (1965) Evidence discriminating between the chemical and the chemiosmotic mechanisms of electron transport phosphorylation. *Nature 208*, 1205-1206.

2. Schultz, B. E., and Chan, S. I. (2001) Structures and proton-pumping strategies of mitochondrial respiratory enzymes. *Annu. Rev. Biophys. Biomol. Struct. 30*, 23-65.

3. DiMauro, S., and Schon, E. A. (2003) Mitochondrial respiratory-chain diseases. *N. Engl. J. Med. 348*, 2656-2668.

4. Elston, T., Wang, H., and Oster, G. (1998) Energy transduction in ATP synthase. *Nature 391*, 510-514.

5. Fato, R., Bergamini, C., Leoni, S., and Lenaz, G. (2008) Mitochondrial production of reactive oxygen species: Role of complex I and quinone analogues. *Biofactors 32*, 31-39.

6. Fridovich, I. (1999) Fundamental aspects of reactive oxygen species, or what's the matter with oxygen? *Ann. N. Y. Acad. Sci. 893*, 13-18.

7. Matés, J. M., Pérez-Gómez, C., and De Castro, I. N. (1999) Antioxidant enzymes and human diseases. *Clin. Biochem. 32*, 595-603.

8. Armstrong, J. S., Khdour, O., and Hecht, S. M. (2010) Does oxidative stress contribute to the pathology of Friedreich's ataxia? A radical question. *FASEB J. 24*, 2152-2163.

9. Murphy, M. P. (2009) How mitochondria produce reactive oxygen species. *Biochem. J. 417*, 1-13.

10. Barja, G., and Herrero, A. (1998) Localization at complex I and mechanism of the higher free radical production of brain nonsynaptic mitochondria in the short-lived rat than in the longevous pigeon. *J. Bioenerg. Biomembr. 30*, 235-243.

11. St-Pierre, J., Buckingham, J. A., Roebuck, S. J., and Brand, M. D. (2002) Topology of superoxide production from different sites in the mitochondrial electron transport Chain. *J. Biol. Chem. 277*, 44784-44790.

12. Barja, G. (1999) Mitochondrial oxygen radical generation and leak: sites of production in states 4 and 3, organ specificity, and relation to aging and longevity. *J. Bioenerg. Biomembr. 31*, 347-366.

13. Gus' kova, R. A., Ivanov, I. I., Kol'tover, V. K., Akhobadze, V. V., and Rubin, A. B. (1984) Permeability of bilayer lipid membranes for superoxide radicals. *Biochim. Biophys. Acta 778*, 579-585.

14. Cadenas, E., and Davies, K. J. A. (2000) Mitochondrial free radical generation, oxidative stress, and aging. *Free Rad. Biol. Med. 29*, 222-230.

15. Tirmenstein, M., Nicholls-Grzemski, F., Zhang, J. G., and Fariss, M. (2000) Glutathione depletion and the production of reactive oxygen species in isolated hepatocyte suspensions. *Chem. Biol. Interact. 127*, 201-217.

16. Wallace, D. C., Fan, W., and Procaccio, V. (2010) Mitochondrial energetics and therapeutics. *Annu. Rev. Pathol. Mech. Dis. 5*, 297-348.

17. Devun, F., Walter, L., Belliere, J., Cottet-Rousselle, C., Leverve, X., Fontaine, E., and Lewin, A. (2010) Ubiquinone analogs: a mitochondrial permeability transition pore-dependent pathway to selective cell death. *PloS One 5*, 2640-2647.

18. Kelso, G. F., Porteous, C. M., Coulter, C. V., Hughes, G., Porteous, W. K., Ledgerwood, E. C., Smith, R. A. J., and Murphy, M. P. (2001) Selective targeting of a redox-active ubiquinone to mitochondria within cells. *J. Biol. Chem. 276*, 4588-4596.

19. López, L. C., Quinzii, C. M., Area, E., Naini, A., Rahman, S., Schuelke, M., Salviati, L., DiMauro, S., Hirano, M., and Andreu, A. L. (2010) Treatment of CoQ_{10} deficient fibroblasts with ubiquinone, CoQ analogs, and vitamin c: time and compound-dependent effects. *PloS One 5*, 473-487.

20. Lenaz, G., Samori, B., Fato, R., Battino, M., Parenti Castelli, G., and Domini, I. (1992) Localization and preferred orientations of ubiquinone homologs in model bilayers. *Biochem. Cell Biol. 70*, 504-514.

21. Meier, T., and Buyse, G. (2009) Idebenone: an emerging therapy for Friedreich ataxia. *J. Neurol. 256*, 25-30.

22. Geromel, V., Darin, N., Chrétien, D., Bénit, P., DeLonlay, P., Rötig, A., Munnich, A., and Rustin, P. (2002) Coenzyme Q10 and idebenone in the therapy of respiratory chain diseases: rationale and comparative benefits. *Mol. Genet. Metab. 77*, 21-30.

23. Telford, J. E., Kilbride, S. M., and Davey, G. P. (2010) Decylubiquinone increases mitochondrial function in synaptosomes. *J. Biol. Chem. 285*, 8639-8645.

24. Lenaz, G. (1998) Quinone specificity of complex I. *Biochim. Biophys. Acta 1364*, 207-221.

25. Hano, N., Nakashima, Y., Shinzawa-Itoh, K., and Yoshikawa, S. (2003) Effect of the side chain structure of coenzyme Q on the steady state kinetics of bovine heart NADH: coenzyme Q oxidoreductase. *J. Bioenerg. Biomembr. 35*, 257-265.

26. James, A. M., Sharpley, M. S., Manas, A. R. B., Frerman, F. E., Hirst, J., Smith, R. A. J., and Murphy, M. P. (2007) Interaction of the mitochondria-targeted antioxidant MitoQ with phospholipid bilayers and ubiquinone oxidoreductases. *J. Biol. Chem. 282*, 14708-14718.

27. Lin, M. T., and Beal, M. F. (2006) Mitochondrial dysfunction and oxidative stress in neurodegenerative diseases. *Nature 443*, 787-795.

28. Calabrese, V., Lodi, R., Tonon, C., D'Agata, V., Sapienza, M., Scapagnini, G., Mangiameli, A., Pennisi, G., Stella, A., and Butterfield, D. A. (2005) Oxidative stress, mitochondrial dysfunction and cellular stress response in Friedreich's ataxia. *J. Neurol. Sci. 233*, 145-162.

29. Tan, G., Chen, L. S., Lonnerdal, B., Gellera, C., Taroni, F. A., and Cortopassi, G. A. (2001) Frataxin expression rescues mitochondrial dysfunctions in FRDA cells. *Hum. Mol. Genet. 10*, 2099-2107.

30. Condò, I., Ventura, N., Malisan, F., Tomassini, B., and Testi, R. (2006) A pool of extramitochondrial frataxin that promotes cell survival. *J. Biol. Chem. 281*, 16750-16756.

31. Campuzano, V., Montermini, L., Molto, M. D., Pianese, L., Cossee, M., Cavalcanti, F., Monros, E., Rodius, F., Duclos, F., and Monticelli, A. (1996) Friedreich's ataxia: autosomal recessive disease caused by an intronic GAA triplet repeat expansion. *Science 271*, 1423-1427.

32. Cooper, J., and Schapira, A. (2007) Friedreich's ataxia: coenzyme Q10 and vitamin E therapy. *Mitochondrion 7*, S127-S135.

33. Gakh, O., Bedekovics, T., Duncan, S. F., Smith, D. Y., Berkholz, D. S., and Isaya, G. (2010) Normal and Friedreich ataxia cells express different isoforms of frataxin with complementary roles in iron-sulfur cluster assembly. *J. Biol. Chem. 285*, 38486-38501.

34. Jauslin, M. L., Wirth, T., Meier, T., and Schoumacher, F. (2002) A cellular model for Friedreich ataxia reveals small-molecule glutathione

peroxidase mimetics as novel treatment strategy. *Hum. Mol. Genet. 11*, 3055-3063.

35. Altman, S. A., Randers, L., and Rao, G. (1993) Comparison of trypan blue dye exclusion and fluorometric assays for mammalian cell viability determinations. *Biotechnol. Prog. 9*, 671-674.

36. Pommier, Y. (2006) Topoisomerase I inhibitors: camptothecins and beyond. *Nat. Rev. Cancer 6*, 789-802.

37. Thomas, C. J., Rahier, N. J., and Hecht, S. M. (2004) Camptothecin: current perspectives. *Bioorg. Med. Chem. 12*, 1585-1604.

38. Graille, M., Cladičre, L., Durand, D., Lecointe, F., Gadelle, D., Quevillon-Cheruel, S., Vachette, P., Forterre, P., and van Tilbeurgh, H. (2008) Crystal structure of an intact type II DNA topoisomerase: insights into DNA transfer mechanisms. *Structure 16*, 360-370.

39. Berger, J. M., and Wang, J. C. (1996) Recent developments in DNA topoisomerase II structure and mechanism. *Curr. Opin. Struct. Biol. 6*, 84-90.

40. Stevnsner, T., Mortensen, U. H., Westergaard, O., and Bonven, B. (1989) Interactions between eukaryotic DNA topoisomerase I and a specific binding sequence. *J. Biol. Chem. 264*, 10110-10113.

41. Edwards, K. A., Halligan, B. D., Davis, J. L., Nivera, N. L., and Liu, L. F. (1982) Recognition sites of eukaryotic DNA topoisomerase I: DNA nucleotide sequencing analysis of topo I cleavage sites on SV40 DNA. *Nucleic Acids Res. 10*, 2565-2576.

42. Denny, W. A., and Baguley, B. C. (2003) Dual topoisomerase I/II inhibitors in cancer therapy. *Curr. Top. Med. Chem. 3*, 339-353.

43. Hsiang, Y. H., Hertzberg, R., Hecht, S., and Liu, L. (1985) Camptothecin induces protein-linked DNA breaks via mammalian DNA topoisomerase I. *J. Biol. Chem. 260*, 14873-14878.

44. Rasheed, Z. A., and Rubin, E. H. (2003) Mechanisms of resistance to topoisomerase I-targeting drugs. *Oncogene 22*, 7296-7304.

45. Hertzberg, R. (1989) Modification of the hydroxyl lactone ring of camptothecin-inhibition of mammalian topoisomerase-I and biological activity. *J. Med. Chem. 32*, 715-720.

46. Jaxel, C. (1989) Structure-activity study of the actions of camptothecin derivatives on mammalian topoisomerase-I evidence for a specific receptor-site and relation to antitumor-activity. *Cancer Res. 49*, 1465-1469.

47. Mi, Z., and Burke, T.G. (1994) Differential interactions of camptothecin lactone and carboxylate forms with human blood components. *Biochemistry 33*, 10325-10336.

48. Dexheimer, T. S., and Pommier, Y. (2008) DNA Cleavage assays for the identification of topoisomerase I inhibitors. *Nat. Protoc. 3*, 1736-1750.

49. Pommier, Y., Leo, E., Zhang, H. L., and Marchand, C. (2010) DNA topoisomerases and their poisoning by anticancer and antibacterial drugs. *Chem. Biol. 17*, 421-433.

50. Long, B. H., Musial, S. T., and Brattain, M. G. (1985) Single-and double-strand DNA breakage and repair in human lung adenocarcinoma cells exposed to etoposide and teniposide. *Cancer Res. 45*, 3106-3112.

51. Zwelling, L. A., Michaels, S., Erickson, L. C., Ungerleider, R. S., Nichols, M., and Kohn, K. W. (1981) Protein-associated deoxyribonucleic acid strand breaks in L1210 cells treated with the deoxyribonucleic acid intercalating agents 4'-(9-Acridinylamino) methanesulfon-m-anisidide and adriamycin. *Biochemistry 20*, 6553-6563.

52. Fortune, J. M., and Osheroff, N. (2000) Topoisomerase II as a target for anticancer drugs: when enzymes stop being nice. *Prog. Nucleic Acid Res. Mol. Biol. 64*, 221-253.

53. Chen, M., and Beck, W. T. (1995) Differences in inhibition of chromosome separation and G2 arrest by DNA topoisomerase II inhibitors merbarone and VM-26. *Cancer Res. 55*, 1509-1516.

54. Ishida, R., Hamatake, M., Wasserman, R. A., Nitiss, J. L., Wang, J. C., and Andoh, T. (1995) DNA topoisomerase II is the molecular target of bisdioxopiperazine derivatives ICRF-159 and ICRF-193 in Saccharomyces Cerevisiae. *Cancer Res. 55*, 2299-2309.

55. Nitiss, J. L. (2009) Targeting DNA topoisomerase II in cancer chemotherapy. *Nat. Rev. Cancer 9*, 338-350.

56. Husain, I., Mohler, J. L., Seigler, H. F., and Besterman, J. M. (1994) Elevation of topoisomerase I messenger RNA, protein, and catalytic activity in human tumors: demonstration of tumor-type specificity and implications for cancer chemotherapy. *Cancer Res. 54*, 539-550.

57. Holden, J. A., Rolfson, D. H., and Wittwer, C. T. (1990) Human DNA topoisomerase II: evaluation of enzyme activity in normal and neoplastic tissues. *Biochemistry 29*, 2127-2134.

58. Heck, M., Hittelman, W. N., and Earnshaw, W. C. (1988) Differential expression of DNA topoisomerases I and II during the eukaryotic cell cycle. *Proc. Natl. Acad. Sci. U. S. A. 85*, 1086-1090.

59. Wang, S., Miller, W., Milton, J., Vicker, N., Stewart, A., Charlton, P., Mistry, P., Hardick, D., and Denny, W. A. (2002) Structure-activity relationships for analogues of the phenazine-based dual topoisomerase I/II Inhibitor XR11576. *Bioorg. Med. Chem. Lett. 12*, 415-418.

60. Kanai, Y., Ishiyama, D., Senda, H., Iwatani, W., Takahashi, H., Konno, H., Tokumasu, S., and Kanazawa, S. (2000) Novel human topoisomerase I inhibitors, topopyrones A, B, C and D: I. producing strain, fermentation, isolation, physico-chemical properties and biological activity. *J. Antibiot. 53*, 863-872.

61. Ishiyama, D., Kanai, Y., Senda, H., Iwatani, W., Takahashi, H., Konno, H., and Kanazawa, S. (2000) Novel human topoisomerase I inhibitors, topopyrones A, B, C and D: II. structure elucidation. *J. Antibiot. 53*, 873-878.

62. Khan, Q. A., Elban, M. A., and Hecht, S. M. (2008) The topopyrones poison human DNA topoisomerases I and II. *J. Am. Chem. Soc. 130*, 12888-12889.